Determination of the internal quantum efficiency for photoelectrochemical reaction in a semiconductor photoelectrode by photoacoustic detection

doi: https://doi.org/10.1039/D0CC01911A

Determination of the internal quantum efficiency for photoelectrochemical reaction in a semiconductor photoelectrode by photoacoustic detection

Naoya Murakami*[a,b] and Keita Okuzono [b]

[a]Department of Applied Chemistry, Faculty of Engineering, Kyushu Institute of Technology, 1-1 Sensuicho, Tobata, Kitakyushu 804-8550, Japan.

[b]Graduate School of Life Science and Systems Engineering, Kyushu Institute of Technology, 2-4 Hibikino, Wakamatsu-ku, Kitakyushu 808-0196, Japan.

We showed for the first time the validity of photothermal measurement for determination of internal quantum efficiency, which is one of the most fundamental values for energy conversion systems. The measurement method using photoacoustic detection in the present study can be applied to a wide variety of samples and measurement conditions.

Quantum efficiency (QE) is one of the most fundamental values for energy conversion systems using photon energy including solar cells, photoluminescent materials, photocatalysts, and photoelectrodes. QE can be divided into internal quantum efficiency (IQE) and external quantum efficiency (EQE) by its definition. For photoelectrochemical (PEC) systems using n-type and p-type semiconductor electrodes, which can drive thermodynamically uphill reactions using photon energy,[1-9] EQE is frequently estimated because it is important from the viewpoint of applications. EQE is calculated as a number ratio of current flowing through the circuit to incident photons, and it is called incident photon-to-current conversion efficiency (IPCE). Although EQE can be estimated easily, only EQE data are not sufficient to discuss whether photoabsorption rate or reaction rate separately have a large influence on PEC performance. On the other hand, IQE is calculated as a number ratio of current flowing through the circuit to absorbed photons, and it is called absorbed photon-to-current conversion efficiency (APCE). Therefore, reaction rate can be discussed separately from absorption rate if IQE data are available. However, it is almost impossible to determine the number of absorbed photons for a solid sample due to light scattering unless the sample is transparent. Therefore, estimation of IQE is not easy in the case of a porous electrode with a large surface area, and there have been few studies showing IQE data for a transparent photoelectrode calculated by light harvesting efficiency (LHE).

A method for determination of IQE for a PEC reaction over a semiconductor electrode using photothermal detection was first reported at the end of the 1970s,[10] and the applicability of this method for IQE determination has been supported by results of subsequent studies.[11-25] In this method, joule heat generated by a current flowing in a depletion layer region is analysed as a function of applied potential, and IQE can be determined by the intercept of the obtained graph. This photothermal detection can be applied to opaque and strongly light-scattering materials because the absorbed photon energy is evaluated thorough heat generated by photoexcitation. Moreover, measurement of light intensity is not required. However, experimental evidence for the validity of this method has not been shown by a comparison of conventional and photothermal methods for a transparent sample, though some studies have shown a comparison between IQE and EQE.[11-13]

Here, we show experimental evidence of the validity of IQE measurement using a transparent semiconductor film on a transparent conductive substrate. In previous studies, the photothermal signal was detected by attaching a thermistor,[10-15] piezoelectric sensor,[16,17] microphone[18-20] or pyroelectric sensor[21-23] on the back side of an opaque sample, i.e., direct coupling method. However, the detection cannot be applied to semitransparent ~ transparent samples because background noise is increased by light transmitted through the sample. Although the photothermal deflection method[24,25] can be applied to such a sample, it is difficult to avoid upsizing of the optical system and

optical adjustment. In contrast, photoacoustic (PA) detection,[26,27] which is one of the photothermal detection methods, can be applied to various kinds of samples including transparent, semitransparent and opaque samples if a gas-microphone PA cell, in which the sample and microphone are spatially separated in order to avoid the influence of transmitted and scattered light, is utilized. We have developed a PA spectroscopic system for evaluation of photocatalytic materials using a micro-electro mechanical system (MEMS) microphone.[28-30] This system enables measurement with high stability under various conditions. In the present study, we carried out PEC and PA measurements of a transparent bismuth vanadate ($BiVO_4$) electrode simultaneously, and we compared IQE determined from PA measurement with IQE derived from EQE and LHE. This is the first report showing the validity of IQE measurement of PEC by photothermal detection.

A $BiVO_4$ film as an n-type semiconductor was deposited on a fluorine-doped tin oxide-coated glass (FTO glass) substrate by the metal organic decomposition (MOD) technique.[3,7] Typically, commercial MOD solutions for bismuth oxide and vanadium oxide were mixed, and butyl acetate and ethyl cellulose were added. The solution was coated on FTO glass (Geomatec, 10 ohm/sq, 0.5 mmt) with a spin-coater, and it was heat-treated using an electric furnace at 500°C for 30 min. The samples prepared without and with ethyl cellulose are denoted as wo-EC and w-EC, respectively. LHE of the prepared transparent sample was estimated using a homemade spectroscopic system (Fig. S1), which was customized to minimize the influence of light scattering on a $BiVO_4$/FTO sample.

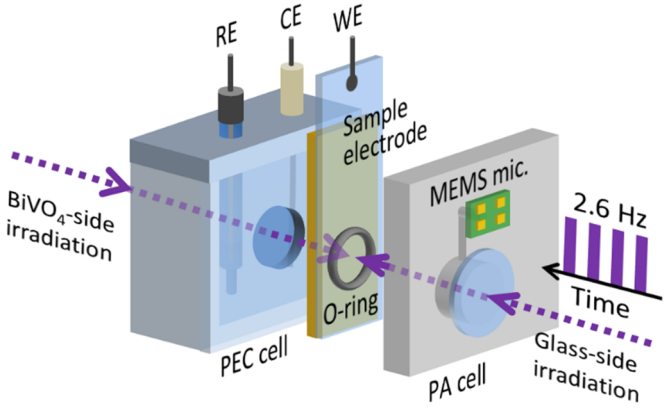

Fig. 1 Schematic illustration of the system for simultaneous PEC and PA measurements.

PEC measurement using a three-electrode type cell (Ag/AgCl as a reference electrode and Pt as a counter electrode) and a potentiostat (Princeton Applied Research, 263A) equipped with a lock-in amplifier (Stanford Research Systems, SR830) and PA measurement were carried out simultaneously. The electrolyte used was 0.1 mol/L Na_2SO_3 + 0.1 mol/L Na_2SO_4 (pH 9.5). A homemade PA cell with an acrylic body and a quartz window was used. For PEC measurements, the PA cell was attached to

the back side (glass side) of a sample electrode, and photoirradiation was carried out from the glass side or $BiVO_4$ film side. A laser diode module (Edmund Optics, 85-227, 405 nm, 10.2 mW) was used as the light source, and the output intensity was modulated at 2.6 Hz. A schematic image of the measurement system is shown in Fig. 1.

Fig. S3 shows a photograph of $BiVO_4$/FTO. For the wo-EC sample, transparency was observed, while lower transparency and a deeper yellow colour were observed for the w-EC sample, indicating that w-EC has porous thicker films. Since the wo-EC sample has high transparency, transmittance/reflectance (T/R) measurement was carried out. From transmittance for FTO glass and $BiVO_4$/FTO, transmittance values of $BiVO_4$ (T_{BiVO4}) was calculated from equation (1).

$$T_{BiVO4} = T_{BiVO4/FTO} / T_{FTO} \quad (1)$$

where T_{FTO} and $T_{BiVO4/FTO}$ are transmittance values of FTO glass and a $BiVO_4$/FTO sample. In the case of LHE for glass-side irradiation, LHE of the prepared $BiVO_4$ film can be calculated from equation (2).

$$LHE = T_{FTO} (1 - T_{BiVO4} - R_{glass\text{-}side}) \quad (2)$$

where $R_{glass\text{-}side}$ is reflectance between $BiVO_4$ and FTO, and it was calculated using the reflective indices of FTO (2.0) and $BiVO_4$ (2.8).[31]

In the case of LHE for $BiVO_4$-side irradiation, LHE of the prepared $BiVO_4$ film can be calculated from equation (3).

$$LHE = 1 - T_{BiVO4} - R_{BiVO4\text{-}side} \quad (3)$$

where $R_{BiVO4\text{-}side}$ is reflectance between $BiVO_4$ and air, and it was estimated from reflectance of a $BiVO_4$/FTO sample by $BiVO_4$-side incidence. LHE values of the prepared $BiVO_4$ film by glass-side incidence and $BiVO_4$-side incidence were estimated to be 25.7% and 13.8%, respectively. The reason why LHE value by glass-side incidence was larger than that by $BiVO_4$-side incidence can be explained by much larger value of $R_{BiVO4\text{-}side}$ than $R_{glass\text{-}side}$, which is caused from difference between two refractive indices of materials at the interface (air/$BiVO_4$ and FTO/$BiVO_4$). The estimation of LHE was carried out in an air atmosphere, while PEC reaction was measured in the aqueous electrolyte solution. Therefore, IQE derived from EQE and LHE (described later) includes a slight error.

As shown in previous studies, a $BiVO_4$ electrode as an n-type semiconductor is known to show a photoanodic current under an appropriate bias condition. Fig. 2a shows the photocurrent of a

$BiVO_4$/FTO electrode (wo-EC sample, glass-side irradiation). The photocurrent increased and then showed an saturation tendency as an applied potential, and average EQE was calculated to be 9.3% in the limiting photocurrent region of 0.4 ~ 0.8 V using the following equation.

$$EQE = (1240 \times j_{ph}) / (\lambda \times P) \quad (4)$$

where j_{ph} is photocurrent, λ is incident wavelength, and P is the intensity of incident light to the $BiVO_4$/FTO sample. Therefore, average IQE was calculated to be 36.3% from LHE of 25.7% using the following equation.

$$IQE = EQE / LHE \quad (5)$$

Fig. 2b shows $E(\Delta P/\Delta P_0)$ as a function of applied potential. When the electrode is illuminated with a light having an energy E with an average absorbed intensity I for time t, the following equation can be obtained by considering the energy balance within the electrode.[10-17]

$$E(\Delta P/\Delta P_0) = (Q_{sc} + T\Delta S)/(I\,t) + \eta(V - V_{fb}) \quad (6)$$

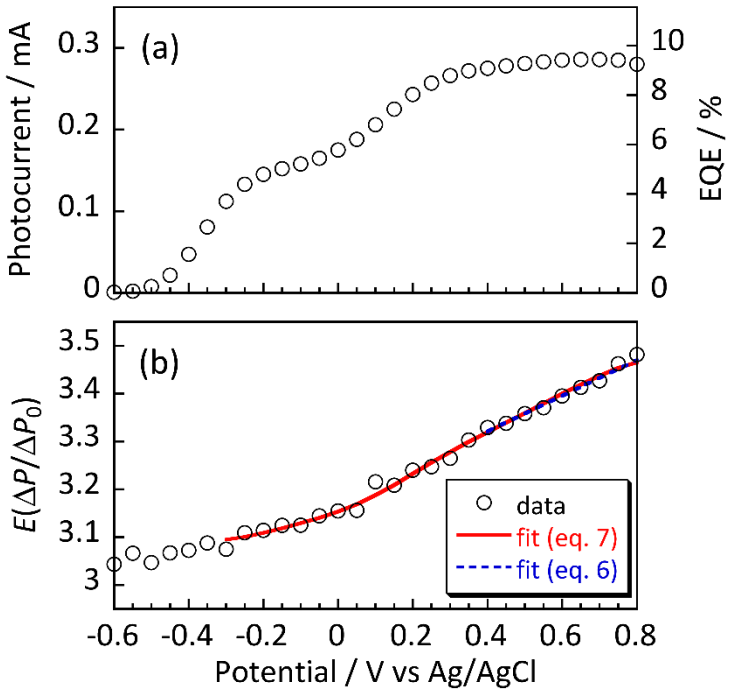

Fig. 2 (a) Photocurrent and (b) $E(\Delta P/\Delta P_0)$ of a $BiVO_4$/FTO electrode (wo-EC sample, glass-side irradiation) in aqueous Na_2SO_3+Na_2SO_4 electrolyte as a function of applied potential.

where ΔP is PA intensity with an applied potential V, ΔP_0 is PA intensity for an open circuit, Q_{sc} is the heat evolved, ΔS is the entropy change, and V_{fb} is flat-band potential. In the limiting photocurrent region, a plot of $E(\Delta P/\Delta P_0)$ against $(V - V_{fb})$ yields the IQE, η, from the slope of the straight line. In the limiting photocurrent region of 0.4 ~ 0.8 V (Fig. 2b), η of 37.3% was obtained from the slope of the straight line, and the η value coincides with IQE calculated from EQE and LHE. The result indicates that PA measurement in the present study is valid for IQE determination of a PEC system using a photoelectrode.

Moreover, we expand this method in order to make it applicable even in the case of no appearance of a plateau region in photocurrent curves. Here, we used $\eta(V)$ instead of the constant value η, which means η is function of V. Because $(Q_{sc} + T\Delta S)/(It)$ is also expressed as a linear function of $\eta(V)$, which is directly proportional to photocuurent $j_{ph}(V)$, we can obtained the following modified equation,

$$E(\Delta P/\Delta P_0) = (C_1 j_{ph}(V) + C_2) + C_3 j_{ph}(V) (V - V_{fb}) \qquad (7)$$

where C_1, C_2 and C_3 are constant values and $C_1 j_{ph}(V) + C_2 = (Q_{sc} + T\Delta S)/(I t)$ and $C_3 j_{ph}(V) = \eta$. In the region of $>V_{fb}$, C_1, C_2 and C_3 can be determined by curve fitting of Fig. 2b using equation (7) and photocurrent data in Fig. 2a as $j_{ph}(V)$. By using this method, the average value of $\eta(V)$ at 0.4 ~ 0.8 V was estimated to be 36.0%, and it agrees with the η value estimated by the previous method (37.3%) and IQE calculated from EQE and LHE (36.3%). The results indicate that the method using curve fitting with equation (7) is applicable to determination of IQE even in the case of no appearance of a plateau region.

We carried out the same experiment with change only in the irradiation direction because PEC performance depends on the irradiation direction as a result of differences in photoabsorption and/or diffusion lengths of electrons and positive holes. In general, a long migration distance of electrons is preferable to that of positive holes for an efficient PEC reaction over an n-type semiconductor. Fig. S4 shows the photocurrent and $E(\Delta P/\Delta P_0)$ of a $BiVO_4$ electrode (wo-EC sample, $BiVO_4$-side irradiation) as a function of applied potential. Although EQE and IQE differed depending on the irradiation direction (glass-side or $BiVO_4$-side irradiation) as expected, IQE estimated from PA measurement coincided with IQE obtained from EQE and LHE. The reason for the higher IQE for $BiVO_4$-side irradiation is that positive holes generated close to the electrolyte interface were utilized in oxidation, and electrons, which have a longer diffusion length, reached the FTO substrate.

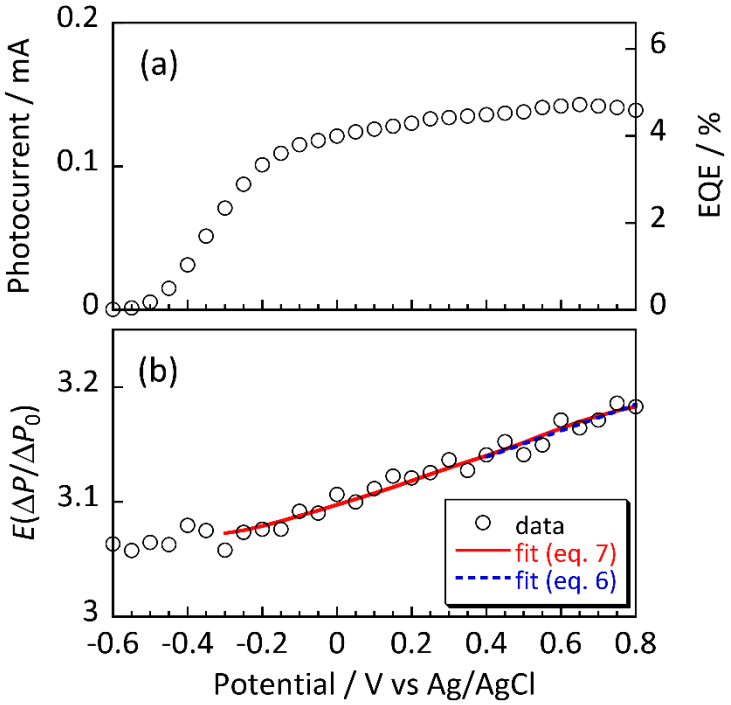

Fig. 3 (a) Photocurrent and (b) $E(\Delta P/\Delta P_0)$ of a $BiVO_4$/FTO electrode (w-EC sample, glass-side irradiation) in aqueous Na_2SO_3+Na_2SO_4 electrolyte as a function of applied potential.

Finally, in order to show the applicability for a semi-transparent sample, a w-EC sample was also measured in the same manner. Fig. 3 shows the photocurrent and $E(\Delta P/\Delta P_0)$ of a $BiVO_4$ electrode (w-EC sample, glass-side irradiation) as a function of applied potential. Even for a semi-transparent sample, results similar to those shown in Fig. 2 were obtained, and EQE and η were calculated to be 4.6% and 10.3%, respectively, in the limiting photocurrent region of 0.4 ~ 0.8 V of Fig. 3, respectively. Therefore, LHE of the sample was calculated to be 44.7% using equation (5), and the LHE value was

Table 1 Summary of T/R, photocurrent and PA measurements.

Sample	transparency	Irradiation direction	[a]LHE /%	[b]EQE /%	[c]IQE /%	[d]η /%	[e]η /%
wo-EC	completely	glass-side	25.7	9.3	36.3	37.3	36.0
wo-EC	completely	$BiVO_4$-side	13.8	5.9	42.5	40.2	40.9
w-EC	semi-	glass-side	–	4.6	–	11.4	10.3

[a]LHE was estimated from T/R measurements using equations (1) ~ (3). [b]EQE was calculated using equation (4). [c]IQE was calculated from EQE and LHE using equation (5). [d]η was calculated using equation (6). [e]η was calculated using equation (7) EQE, IQE and η are the average values at 0.4 ~ 0.8 V vs Ag/AgCl of applied potential.

larger than that of the wo-EC sample. These are reasonable results because a thick film was observed from the appearance (Fig. S3).

The present study showed for the first time the validity of IQE measurement of PEC over a semiconductor photoelectrode by means of photothermal detection using PA detection. The system used in the present study has various advantages over the systems used in previous studies. The advantages include (1) applicability for a sample with semi-transparency and low IQE, (2) no requirement for a high applied potential and light source emitting high-intensity and short-wavelength light, and (3) easy attachment of the PA cell to a sample electrode and easy detachment from the electrode. As a future prospect, IQE determination might be possible by correction using PA intensity attributed to an electrocatalyst even if it possesses light absorption. A new method using curve fitting, which enables IQE determination even if a plateau was not observed, was also proposed. We are now ready for the next step, i.e., measurements of action spectra (dependence of wavelength on incident light) of IQE for elucidation of the mechanism of a PEC reaction over a photoelectode.

This work was supported by a Grant-in-Aid for Scientific Research on Innovative Areas “Innovations for Light-Energy Conversion (I4LEC)” (Grant Number 18H05172).

Conflicts of interest

There are no conflicts to declare.

Notes and references

1 A. Fujishima, K. Honda, *Nature*, 1972, **238**, 37–38.

2 T. Hisatomi, J. Kubota, K. Domen, *Chem. Soc. Rev.*, 2014, **43**, 7520–7535.

3 K. Fuku, K. Sayama, *Chem. Commun.*, 2016, **52**, 5406–5409.

4 T. Arai, S. Sato, K. Sekizawa, T.M. Suzuki, T. Morikawa, *Chem. Commun.*, 2019, **55**, 237–240.

5 C.D. Windle, H. Kumagai, M. Higashi, R. Brisse, S. Bold, B. Jousselme, M. Chavarot-Kerlidou, K. Maeda, R. Abe, O. Ishitani, V. Artero, *J. Am. Chem. Soc.*, 2019, **141**, 9593–9602.

6 Y. Kageshima, Y. Goto, H. Kaneko, M. Nakabayashi, N. Shibata, K. Domen, T. Minegishi, *ChemCatChem*, 2019, **11**, 4266–4271.

7 H. Tateno, Y. Miseki, K. Sayama, *Chem. Commun.*, 2019, **55**, 9339–9342.

8 S. Ikeda, S. Fujikawa, T. Harada, T.H. Nguyen, S. Nakanishi, T. Takayama, A. Iwase, A. Kudo, *ACS Appl. Energy Mater.*, 2019, **2**, 6911–6918.

9 I. Tomoya, H. Masanobu, I. Shigeru, A. Yutaka, *ChemCatChem*, 2019, **11**, 6227–6235.

10 A. Fujishima, Y. Maeda, K. Honda, G.H. Brilmyer, A.J. Bard, *J. Electrochem. Soc.*, 1980, **127**, 840–846.

11 Y. Maeda, A. Fujishima, K. Honda, *Chem. Lett.*, 1980, **9**, 271–274.

12 A. Fujishima, Y. Maeda, K. Honda, *Bull. Chem. Soc. Jpn.*, 1980, **53**, 2735–2741.

13 A. Fujishima, Y. Maeda, S. Suzuki, K. Honda, *Chem. Lett.*, 1982, **11**, 179–182.

14 Y. Maeda, A. Fujishima, K. Honda, *Bull. Chem. Soc. Jpn.*, 1982, **55**, 3373–3376.

15 Y. Maeda, K. Koshi, T. Kato, *J. Electroanal. Chem.*, 1997, **424**, 213–216.

16 S. Yoshihara, A. Fujishima, *Mater. Res. Bull.*, 1988, **23**, 759–763.

17 S. Yoshihara, A. Aruchamy, A. Fujishima, *Bull. Chem. Soc. Jpn.*, 1988, **61**, 1017–1019.

18 J. Rappich, J.K. Dohrmann, *Ber. Bunsenges. Phys. Chem.*, 1988, **92**, 1342–1345.

19 J. Rappich, J.K. Dohrmann, *J. Phys. Chem.*, 1989, **93**, 5261–5264.

20 J. Rappich, J.K. Dohrmann, *J. Phys. Chem.*, 1990, **94**, 7735–7739.

21 J.K. Dohrmann, N. Schaaf, *J. Phys. Chem.*, 1992, **96**, 4558–4563.

22 N. Schaaf, I. Hahndorf, J.K. Dohrmann, *J. Electroanal. Chem.*, 1995, **395**, 173–179.

23 J.K. Dohrmann, M. Chuan, N. Schaaf, *Sol. Energy Mater. Sol. Cells*, 1996, **43**, 273–296.

24 R.E. Wagner, A. Mandelis, *Phys. Rev. B*, 1988, **38**, 9920–9927.

25 P. Grunow, J. Rappich, J.K. Dohrmann, *J. Electroanal. Chem.*, 1992, **337**, 181–186.

26 A. Rosencwaig, A. Gersho, *J. Appl. Phys.*, 1976, **47**, 64−69.

27 A.C. Tam, *Rev. Mod. Phys.*, 1986, **58**, 381−431.

28 N. Murakami, T. Shinoda, *J. Phys. Chem. C*, 2019, **123**, 222–226.

29 T. Shinoda, N. Murakami, *J. Phys. Chem. C*, 2019, **123**, 12169–12175.

30 N. Murakami, T. Shinoda, *Phys. Chem. Chem. Phys.*, 2018, **20**, 24519–24522.

31 Z. Zhao, Z. Li, Z. Zou, Phys. *Chem. Chem. Phys.*, 2011, **13**, 4746–4753